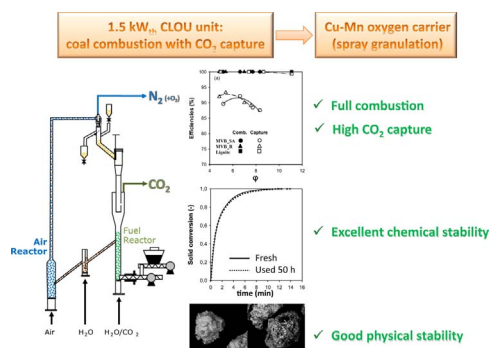Full Length Article

CLOU process performance with a Cu-Mn oxygen carrier in the combustion of different types of coal with CO_2 capture

Iñaki Adánez-Rubio, Alberto Abad*, Pilar Gayán, Luis F. de Diego, Juan Adánez

Instituto de Carboquímica (ICB-CSIC), Dept. of Energy & Environment, Miguel Luesma Castán, 4, Zaragoza 50018, Spain

GRAPHICAL ABSTRACT

ARTICLE INFO

ABSTRACT

The Chemical Looping with Oxygen Uncoupling (CLOU) process is a Chemical Looping Combustion (CLC) technology that allows the combustion of solid fuels with inherent CO_2 separation by using oxygen carriers based on metal oxides. This technology has a low energy penalty and thus low CO_2 capture costs. The oxygen carrier used in the CLOU process must be able to release gaseous oxygen, an aspect that limits the availability of metal oxides for this process. This work investigated the suitability of an oxygen carrier containing 34 wt% CuO and 66 wt% Mn_3O_4 (active phase $Cu_{1.5}Mn_{1.5}O_4$) prepared by granulation regarding the CO_2 capture, combustion efficiency and lifetime of the particles. The effect of the different types of coal (two sub-bituminous and a lignite) on combustion and CO_2 capture efficiencies by CLOU was studied at different oxygen carrier to coal ratios in a continuous $1.5\,kW_{th}$ rig. It was found that full combustion could be reached regardless of the coal used. However, CO_2 capture efficiencies were highly determined by coal rank. Finally, it was found that working with oxygen carrier to coal ratios higher than $\phi = 4$, which corresponded to values of the variation of the oxygen carrier conversion lower than $\Delta X_{oc} = 0.25$, decreased the effect of chemical stress on the attrition rate. Therefore, it is clearly beneficial for the lifetime of oxygen carrier particles to operate with low variations of the oxygen carrier conversion (ΔX_{oc}) between fuel and air reactors.

1. Introduction

A promising Chemical Looping Combustion (CLC) option for burning solid fuel is the Chemical Looping with Oxygen Uncoupling (CLOU) process. Metallic oxides used as oxygen carriers for the CLOU process must be able to release gaseous oxygen at operating temperatures. The O_2 (g) released by the oxygen carrier in the fuel reactor directly burns the solid fuel fed into it. In addition, the oxygen carrier for

---

Nomenclature

Symbols

F_i	Molar flow of compound i (mol/s)
$f_{C,fix}$	Mass fraction of fix carbon in coal (–)
M_i	Atomic or molecular weight of i elements or compound (kg/mol)
m	Mass of the sample at each time in TGA (kg)
m_{5h}	Mass of fines after 5 h collected from the attrition test rig (kg)
m_s	Mass of sample loaded into the apparatus (kg)
$\dot{m}_{coal}$	Mass-based flow of coal fed-in to the fuel reactor (kg/s)
$\dot{m}_{OC}$	Solids circulation rate (kg/s)
m_{ox}	Mass of the fully oxidized oxygen carrier sample (kg)
$m_{s,FR}$	Mass of solids in the fuel reactor (kg)
m_{FR}^*	Specific solids inventory in the fuel reactor (kg/MW$_{th}$)
R_{OC}	Oxygen transport capability (–)
T	Temperature (°C)
$X_{char,FR}$	Char conversion in the fuel reactor (–)
X_{red}	Oxygen carrier conversion for the reduction reaction (–)

Greek letters

ΔX_{oc}	Variation of the oxygen carrier conversion (–)

η_{CC}	CO_2 capture efficiency (–)
$\eta_{comb,FR}$	Combustion efficiency in the fuel reactor (–)
ϕ	Oxygen carrier to fuel ratio (–)
Ω_{coal}	Stoichiometric mass of O_2 to convert 1 kg of coal (kg/kg)

Acronyms

AJI	Air Jet Index
AR	Air reactor
BET	Brunauer-Emmett-Teller
CLC	Chemical Looping Combustion
CLOU	Chemical Looping with Oxygen Uncoupling
FCC	Fluid catalytic cracking
FR	Fuel reactor
ICP	Inductively coupled plasma
OC	Oxygen carrier
TGA	Thermogravimetric analyser
XRD	X-ray diffractometer

Subscripts

C,elut	Carbon elutriated
outAR	Outlet stream from air reactor
outFR	Outlet stream from fuel reactor

CLOU process must be able to be regenerated by air in the air reactor. Three single metal oxides have the properties required for the CLOU process: CuO/Cu_2O, Mn_2O_3/Mn_3O_4 and Co_3O_4/CoO [1]. Mattisson [2] and Imtiaz et al. [3] conducted reviews of CLOU materials. These reviews included Cu-based oxygen carriers [4,5] and the mixed-oxide-based oxygen carriers Cu-Mn [6,7], Mn-Fe [8] and Mn-Si [9].

Among the developed materials, one consisting of spray dried particles with 60 wt% CuO was analysed in a CLOU unit of 1.5 kW$_{th}$, with it the proof of CLOU concept was demonstrated using different coal ranks and biomass [10–12]. These particles were also used to analyse the fate of sulphur and its effect on CO_2 capture efficiency [13], and the fate of sulphur, nitrogen and mercury was also analysed with a similar oxygen carrier [14]. This Cu-based oxygen carrier did not show any decrease in reactivity or agglomeration. However, it required improvement due to an important reduction in crushing strength and an increase in its porosity [15].

Mn-based oxygen carriers show some advantages with respect to Cu-based materials: they operate at lower temperatures owing to the fact that the partial pressure of O_2 at equilibrium for the Mn_2O_3/Mn_3O_4 is higher than it is for CuO/Cu_2O [1]; and Cu-based materials are more expensive than Mn-based ones. However, the need to decrease the temperature in the air reactor to around 800 °C to regenerate the Mn_3O_4 to Mn_2O_3 makes Mn-based materials unsuitable for use on an industrial scale CLOU process [16–18].

Cu-Mn mixed oxides show good prospects for the CLOU process because they release oxygen at lower temperature than Cu-based oxygen carriers do [7]. A number of works have studied different Cu-Mn oxygen carriers prepared by co-precipitation [7], extrusion [19] and freeze drying [6]. They found that Cu-Mn mixed oxides were able to generate gaseous oxygen above 700 °C and had good reactivity with CH_4, but CO was found to be present in the outlet stream. Depending on the Cu-Mn mixed oxide phase formed during the oxygen carrier preparation, $CuMn_2O_4$ [7,20] or $Cu_{1.5}Mn_{1.5}O_4$ [19,21], oxygen release can occur by means of two different reactions:

$$3CuMn_2O_4 \leftrightarrow 3CuMnO_2 + Mn_3O_4 + O_2 \tag{1}$$

$$2Cu_{1.5}Mn_{1.5}O_4 \leftrightarrow 3CuMnO_2 + O_2 \tag{2}$$

Moreover, an oxygen carrier derived from the commercially prepared hopcalite, Carulite 300®, was analysed as a CLOU oxygen carrier by Adánez-Rubio et al. [21]. It was found that the hopcalite-derived oxygen carrier was able to completely burn coal in the CLOU process to CO_2 and H_2O in a batch fluidized bed reactor at low temperatures. Nevertheless, it showed a reduction in particle crushing strength with the operation time, reaching values under 1 N, which indicated that the physical properties of the particles need improvement. Thus, the oxygen carrier derived from this commercial material was not considered suitable for the CLOU process.

The main efforts currently being made to continue the development of CLOU is to find a suitable oxygen carrier for the process with high mechanical strength and physical stability in order to show low attrition rates, but still having a high oxygen release rate. A new Cu-Mn oxygen carrier for the CLOU process named Cu34Mn66-GR (34 wt% CuO and 66 wt% Mn_3O_4, granulated particles), based on the composition of hopcalite, was developed by our ICB-CSIC research group and prepared by spray granulation [22]. This material showed high reactivity with coal and char in a batch fluidized bed reactor, allowing complete combustion of the coal to CO_2 and H_2O. Moreover, the Cu34Mn66-GR showed an attrition rate (0.005%/h, corresponding to a particle lifetime of 20,000 h) that was 18 times lower than that of the hopcalite-derived oxygen carrier [21]. This material was also tested in a 1.5 kW$_{th}$ continuous CLOU unit burning sub-bituminous Chilean coal, where the effect on combustion and CO_2 capture efficiencies of the fuel reactor temperature, coal feeding rate, solid circulation rate, fluidization agent and O_2 available in the air reactor were analysed [23]. It was found that complete combustion of coal was obtained with fuel reactor temperatures higher than 800 °C. CO_2 capture was higher than 90% at operating temperatures as low as 850 °C in the fuel reactor, reaching 96.2% at 875 °C [23]. On the other hand, the oxygen carrier to fuel ratio (ϕ) is a fundamental parameter for achieving high CO_2 capture efficiencies. Higher ϕ values produced higher char conversion rates in the fuel reactor, because the oxygen generation rate of this oxygen carrier is highly dependent on the reduction conversion. Note that a higher ϕ value resulted in lower reduction conversion, a higher oxygen generation rate, higher char conversion rate and higher CO_2 capture efficiency [22,23]. These results were contrary to what was found for a Cu-based oxygen carrier [10]. The use of steam as a fluidizing agent did not show

any substantial improvement in CO_2 capture efficiency in the process with respect to N_2. Finally, it was found that it was necessary use an air excess ratio of 4 in the air reactor to obtain high CO_2 capture efficiencies [23]. From this previous work, optimized conditions were found for the Cu34Mn66-GR material, namely a fuel reactor temperature of 850 °C, air excess ratio of 4, and oxygen carrier to fuel ratio $\phi > 4$, in order to obtain high CO_2 capture efficiencies.

The aim of this work was to study the effect of high oxygen carrier to fuel ratio values with coals of different rank in a CLOU continuous unit with the oxygen carrier Cu34Mn66-GR under optimized operating conditions. Possible chemical and physical changes in the oxygen carrier particles were evaluated after operation at optimized conditions in order to evaluate the stability of the material.

2. Experimental

2.1. Oxygen carrier

The material used was a Cu-Mn mixed oxide prepared by spray granulation in a spouted bed system. The oxygen carrier particles were manufactured at Instituto de Carboquímica using Mn_3O_4 (STREM, PRS) and CuO (Panreac, PRS) as raw materials. The CuO content was 34 wt% and the Mn_3O_4 was 66 wt%. After formation in a spouted lab unit (Procell, Glatt), the particles were calcined for 2 h at 1125 °C. The oxygen carrier was then given the name Cu34Mn66-GR [22]. Table 1 shows the main properties of this oxygen carrier. The particle size was + 0.1–0.3 mm.

2.2. Oxygen carrier characterization

Physical and chemical characterization of the prepared oxygen carrier (Cu34Mn66-GR) was performed by means of different techniques. Oxygen transport capacity, R_{OC}, was calculated as a function of the composition of the particles after the calcination step. Crushing strength was determined by measuring the force needed to fracture a particle using a Shimpo FGN-5X crushing strength apparatus. Crushing strength was taken as the average value of at least 20 measurements of particles with size diameter between 0.1 to 0.3 mm. For used particles, crushing strength represents the value of the mixture of oxygen carrier, char and ashes present in the fuel reactor. Attrition resistance was determined using a three-hole air jet attrition tester ATTRI-AS (Ma.Tec. Materials Technologies Snc) configured according to the ASTM-D-5757 standard [24]. The weight loss of fines was recorded after 1 h and 5 h of operation, respectively. Eq. (3) shows the air jet index (AJI) value as the percentage of fines after a 5 h test.

$$AJI = \frac{m_{5h}}{m_s} \tag{3}$$

where m_{5h} is the mass of fines after 5 h collected from the attrition test rig, and m_s the mass of sample loaded into the apparatus (nominally 50 g). In the case of the CLOU process, the presence of ashes in the fuel reactor bed together with oxygen carrier particles makes AJI analysis somewhat difficult. After the AJI test, an ICP analysis was carried out on the particles to establish the amount of Cu and Mn from the filter and the bed, which made it possible to ascertain the ash content present both in the recovered and initially tested material.

Skeletal density was determined by He picnometry in a Micromeritics AccuPyc II 1340. The surface area of the oxygen carrier was determined by the Brunauer-Emmett-Teller (BET) method by adsorption/desorption of nitrogen at 77 K in a Micromeritics ASAP-2020 (Micromeritics Instruments Inc.), and pore volume was measured by Hg intrusion in a Quantachrome PoreMaster 33. The identification of crystalline chemical species was carried out by X-ray diffraction (XRD) patterns collected by a Bruker D8 Advance X-ray powder diffractometer, equipped with an X-ray source with a Cu anode working at 40 kV and 40 mA and an energy-dispersive one-dimensional detector.

The diffraction pattern was obtained over the 2θ range of 10° to 80° with a step of 0.019°. The assignation of crystalline phases was performed based on the Joint Committee on Powder Diffraction Standards. DIFFRAC.EVA software was supported by a reference pattern database derived from Crystallography Open Database (COD) and the Powder Diffraction File (PDF) for phase identification. Quantitative XRD analysis of the crystalline phase was performed by Rietveld refinement using TOPAS software.

The main phase determined by XRD was $Cu_{1.5}Mn_{1.5}O_4$, so the mixed oxide was found to have been formed from the separate oxides during the oxygen carrier calcination step. In keeping with composition of the hopcalite-derived oxygen carrier [21], a 2:1 ratio of Mn to Cu was used to prepare the Cu34Mn66-GR particles. As the main phase obtained was $Cu_{1.5}Mn_{1.5}O_4$, the Cu:Mn molar ratio in the active phase was 1:1, thus maintaining an excess of Mn_3O_4 in the particles. However, the oxygen transport capacity for CLOU was reduced, because it is difficult to regenerate Mn_3O_4 to Mn_2O_3 in oxygen carriers based exclusively on Mn oxide [17,25,26] given the low temperature in the air reactor needed for regeneration.

2.3. Coals

Three different coals were used for the CLOU experiments with Cu34Mn66-GR oxygen carrier. A lignite from the Teruel Basin, Spain, and two medium volatile bituminous coals from South Africa (MVB_SA) and Russia (MVB_R) were used with the aim of covering a wide range of coals. The main properties of selected coals (proximate and ultimate analysis and LHV) are shown in Table 2. Note the high ash and sulphur contents of lignite coal. The coal particle size used for this study was + 0.2 to 0.3 mm.

2.4. Experimental setup

A schematic view of the set-up used is shown in Fig. 1. The set-up basically comprised two interconnected fluidized bed reactors – the air and fuel reactors – joined by a loop seal, a riser for solids transport from the air reactor to the fuel reactor, a cyclone and a solids valve to control the solids circulation flow rate in the system. A diverting solids valve located below the cyclone allowed for the measurement of the solids flow rates at any time. This design therefore allowed us to control and measure the solids circulation flow rate between both reactors. A detailed description of the continuous unit can be found in Abad et al. [10].

The fuel reactor temperature was fixed at 850 °C and gas flow was 250 L_N/h, corresponding to a gas velocity of ~ 0.15 m/s. Coal was fed via a twin screw feeder at the bottom of the bed, immediately above the fuel reactor distributor plate, in order to maximize the time that the fuel and volatile matter were in contact with the bed material. A small N_2 flow (24 L_N/h) was introduced at the beginning of the screw feeder to avoid any possible reverse gas flow. Reduced oxygen carrier particles

Table 1
Properties of the Cu-Mn oxygen carrier used in this work: fresh and after 50 h use in continuous operation.
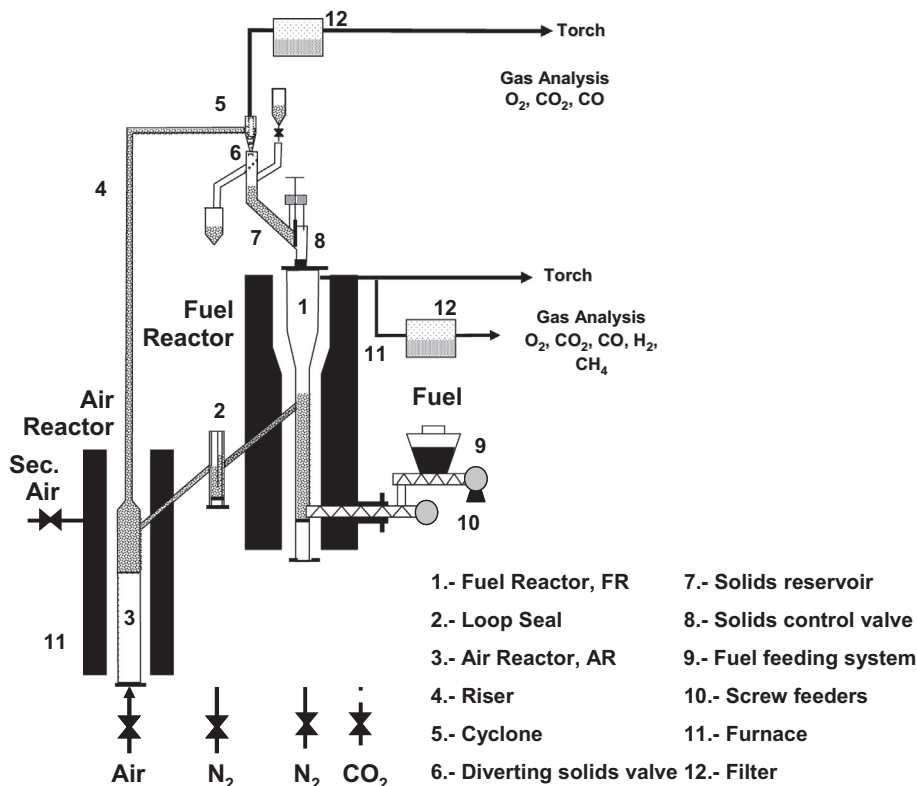
	Fresh	50 h use
XRD main phases	$Cu_{1.5}Mn_{1.5}O_4$, Mn_3O_4	$Cu_{1.5}Mn_{1.5}O_4$, Mn_3O_4, Mn_2O_3
Oxygen transport capacity for CLOU, R_{OC} (wt%)	4.0	4.0
Crushing strength (N)	1.9	1.2
Skeletal density of particles (kg/m^3)	4100	4700
AJI (%)	3.0	7.7
Porosity (%)	12.1	18.7
Specific surface area, BET (m^2/g)	< 0.5	1.0

Table 2
Properties of the coals used in this work.

	Medium Volatile Bituminous (South Africa)	Medium Volatile Bituminous (Russia)	Lignite (Spain)
Proximate analysis (wt%)			
Moisture	4.2	5.8	12.6
Volatile matter	25.5	32.0	28.6
Fixed carbon	55.9	52.1	33.6
Ash	14.4	10.1	25.2
Ultimate analysis (wt%)			
C	69.3	65.8	45.4
H	3.9	4.6	2.5
N	1.9	2.0	0.6
S	0.9	0.5	5.2
O	5.4	11.3	8.5
LHV (kJ/kg)	25,500	26,600	16,250
Ω_{coal} (kg O_2/kg coal)	2.0	1.8	1.2

Table 3
Main data for experimental tests in the CLOU prototype.

Coal	Test	$\dot{m}_{OC}$ (kg/h)	$\dot{m}_{coal}$ (kg/h)	Power (W)	$m_{S,FR}$ (kg)	ϕ	m_{FR}^* (kg/MW$_{th}$)
South Africa	S01	20	0.032	230	1.2	8.3	5200
South Africa	S02	18	0.032	230	1.2	7.7	5200
South Africa	S03	14	0.032	230	1.2	6.6	5200
South Africa	S04	9	0.032	230	1.2	5.2	5200
Russia	R01	20	0.046	340	1.2	7.6	3500
Russia	R02	18	0.046	340	1.2	6.9	3500
Russia	R03	14	0.046	340	1.2	5.4	3500
Russia	R04	12	0.046	340	1.2	4.8	3500
Lignite	L01	18	0.035	160	0.94	11.1	5900
Lignite	L02	15	0.035	160	0.94	8.6	5900
Lignite	L03	13	0.035	160	0.94	7.4	5900
Lignite	L04	8	0.035	160	0.94	4.9	5900

overflowed into the air reactor through fluidized bed loop seal, and a N_2 flow of 90 L_N/h was introduced into the loop seal. Considering the optimized conditions determined for Cu34Mn66-GR [23], the oxidation of the carrier took place in the air reactor with a mixture of air/N_2 flow of 2100 L_N/h (14 vol% O_2 inlet, 8 vol% O_2 outlet). The operation temperature in the air reactor was 800 °C. In addition, a secondary air flow (600 L_N/h) was introduced at the top of the bubbling bed to assist with particle entrainment.

The total oxygen carrier inventory in the system was 3 kg, of which about 1 kg was in the fuel reactor. The CO, CO_2, H_2, CH_4 and O_2 concentrations in the fuel reactor outlet stream and CO, CO_2 and O_2 from the air reactor were continuously recorded. For CH_4, CO and CO_2, a non-dispersive infrared (NDIR) analyser (Siemens Ultramat 23) was used; paramagnetic analysers (Siemens Ultramat 23 and Oxymat 6) were used for O_2 concentration measurement, and a thermal conductivity detector (Siemens Calomat 6) was used for H_2.

2.5. Experimental planning

Table 3 compiles the main variables used in each test. On the whole, the same batch of oxygen carrier particles was used during 50 h of hot fluidization conditions, 25 h of which involved coal combustion. The temperature in the air reactor was fixed at 800 °C; it was selected to optimize the oxidation of the Cu-Mn mixed oxide [23]. The temperature in the fuel reactor was kept stable at 850 °C. To obtain high ϕ values, the coal feeding rate was fixed at low values, and high solids circulation rates were used. The coal feeding rate was varied as a function of the coal type between 0.032 and 0.046 kg/h, which corresponds to a power input of between 230 and 340 W$_{th}$. The solids circulation rate was varied between 8 and 20 kg/h. With these values, the oxygen carrier to fuel ratio, ϕ, was varied from 4.8 to 11.1. ϕ was defined by the following equation [27]:

$$\phi = \frac{\text{Oxygen available in the fully oxidized oxygen carrier}}{\text{Oxygen required by the fuel for full combustion}} \quad (4)$$

Fig. 1. Schematic view of the ICB-CSIC-s1 unit.

1.- Fuel Reactor, FR
2.- Loop Seal
3.- Air Reactor, AR
4.- Riser
5.- Cyclone
6.- Diverting solids valve
7.- Solids reservoir
8.- Solids control valve
9.- Fuel feeding system
10.- Screw feeders
11.- Furnace
12.- Filter

3. Data evaluation

To analyze the performance of the CLOU process, the combustion efficiency in the fuel reactor and the CO_2 capture efficiency were calculated. Calculations are based on the molar flow of every gas analysed, F_i, which is determined from the measured concentration. Mass balances were checked and a closing about 95% was found for the carbon balance. Unbalanced carbon was assumed to be present in unconverted char elutriated from the fuel reactor, $F_{C,elut}$.

The combustion efficiency in the fuel reactor was calculated through the ratio between the oxygen required to fully burn unconverted gases (CH_4, CO and H_2) at the fuel reactor exit and the oxygen demanded by coal converted in the fuel reactor (oxygen to form sulphur or nitrogen oxides was not considered in these calculations). Thus, both the oxygen demanded by the carbon bypassed to the air reactor, $F_{CO_2,AR}$, and elutriated from the fuel reactor, $F_{C,elut}$, are subtracted to the oxygen demanded by coal in the denominator. Therefore, the combustion efficiency in the fuel reactor was calculated as:

$$\eta_{comb,FR} = 1 - \frac{4F_{CH_4,outFR} + F_{CO,outFR} + F_{H_2,outFR}}{\frac{1}{M_{O2}}2\Omega_{coal}\dot{m}_{coal} - 2F_{C,elut} - 2F_{CO_2,outAR}} \qquad (5)$$

The CO_2 capture efficiency, η_{CC}, was defined as the fraction of the carbon converted in the CLC unit which is actually at the outlet of fuel reactor. This is the actual carbon captured in the CLOU system; the remaining is exiting in the air reactor outlet.

$$\eta_{CC} = \frac{F_{CO_2,outFR} + F_{CO,outFR} + F_{CH_4,outFR}}{F_{CO_2,outFR} + F_{CO,outFR} + F_{CH_4,outFR} + F_{CO_2,outAR}} \qquad (6)$$

The CO_2 capture efficiency depends on the conversion of char in the fuel reactor. The conversion of char in the fuel reactor, $X_{char,FR}$, was calculated considering the carbon contained in gases exiting the fuel reactor coming from the char gasified, as well as the carbon not converted in the fuel reactor, which exits as CO_2 from the air reactor or unconverted char elutriated from the fuel reactor.

$$X_{char,FR} = \frac{f_{C,fix} \cdot \dot{m}_{coal} - F_{C,elut} - M_C \cdot F_{CO_2,outAR}}{f_{C,fix} \cdot \dot{m}_{coal} - F_{C,elut}} \qquad (7)$$

4. Results

4.1. Combustion and CO_2 capture efficiency

To investigate the effect of the oxygen carrier to fuel ratio, ϕ, on the CLOU process for the combustion of different rank coals, several test were done in a CLOU continuous unit, ICB-CSIC-s1. Cu34Mn66-GR oxygen carrier prepared by granulation was used. The effect of coal rank and ϕ on the combustion and CO_2 capture efficiencies were investigated. ϕ was varied between 4.8 and 11.1. A total of 50 h of operation was performed in the CLOU continuous unit.

The composition of the gases at the fuel and air reactor outlet streams were determined for every experimental test. By way of example, Fig. 2 shows the gas concentration (dry basis) measured for experiments carried out with Medium Volatile Bituminous coal from Russia. Different ϕ values were tested, and at least 50 min of stable conditions was considered.

When the solid circulation rate was varied to change ϕ, a period of transition appeared and the next stable steady state was reached after around 10 min. At the steady state, the temperature and gas concentration at the outlet stream of both reactors were stable during the whole test. The carbon and oxygen mass balances were accurate (closure > 95%). Therefore, the loss of elutriated char particles from the fuel reactor was negligible. Also, when the steady state was reached, the oxygen transferred from the oxygen carrier to the fuel in the fuel reactor was equal to the oxygen recovered in the air reactor by oxygen carrier oxidation with air.

Fig. 2 shows that there were no unburnt products in the fuel reactor outlet stream. This result was observed for all the coals tested. The only gases present in the fuel reactor outlet were CO_2, H_2O, O_2 and N_2 (introduced as fluidizing agent). Thus, it can be observed in Fig. 2 that the coal volatiles were fully burnt to CO_2 and H_2O in the fuel reactor by means of reaction with the O_2 released by the Cu-Mn mixed oxide reduction. Moreover, the rate of oxygen release was enough to supply an excess of $O_2(g)$ that exited with the combustion gases in the fuel reactor stream. Small fractions of SO_2 and NO were present in the gases coming from the sulphur and nitrogen content of the different coals. However, these compounds were not evaluated in this work.

Combustion and CO_2 capture efficiencies were analysed for all the coals studied, see Fig. 3(a). Complete combustion to CO_2 and H_2O of coal in the fuel reactor was found for all coals and under all experimental conditions used. However, coal rank affects CO_2 capture efficiency. Note that CO_2 capture is related to the carbon exiting the fuel reactor, which proceeds from both volatile matter and converted char. Likely, devolatilization is fast enough to consider that carbon in volatile matter is entirely evolved in the fuel reactor. Thus, the CO_2 capture is mainly affected by the fraction of carbon as fixed carbon and the char conversion in the fuel reactor, which is shown in Fig. 3(b). The highest CO_2 capture efficiency of the lignite fuel is due to its highly reactive char and low fixed carbon content. The similar capture efficiencies of bituminous coals are due to their similar fixed carbon content. However, a lower char conversion for South African coal at lower ϕ values resulted in lower CO_2 capture efficiency at these conditions; see Fig. 3(b).

In order to change the ϕ value and maintain the oxygen carrier inventory in the fuel reactor, the oxygen carrier circulation rate was varied. It was observed with Cu-based oxygen carriers that an increase
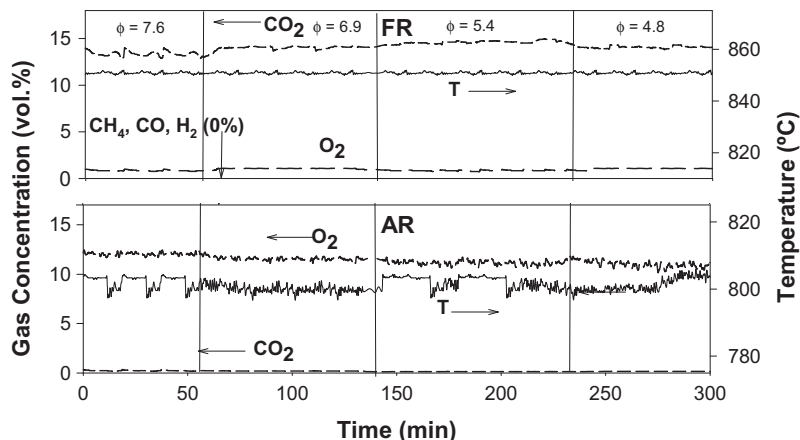

Fig. 2. Evolution of gas composition in the air and fuel reactor as ϕ was varied for Russian MVB coal. Experimental tests R01-R04. $T_{FR} = 850\,°C$; $\dot{m}_{coal} = 0.046$ kg/h.

Fig. 3. (a) Combustion efficiency in the fuel reactor and CO_2 capture efficiency and (b) char conversion in the fuel reactor, as a function of the oxygen carrier to fuel ratio, ϕ, in the combustion of different coals.
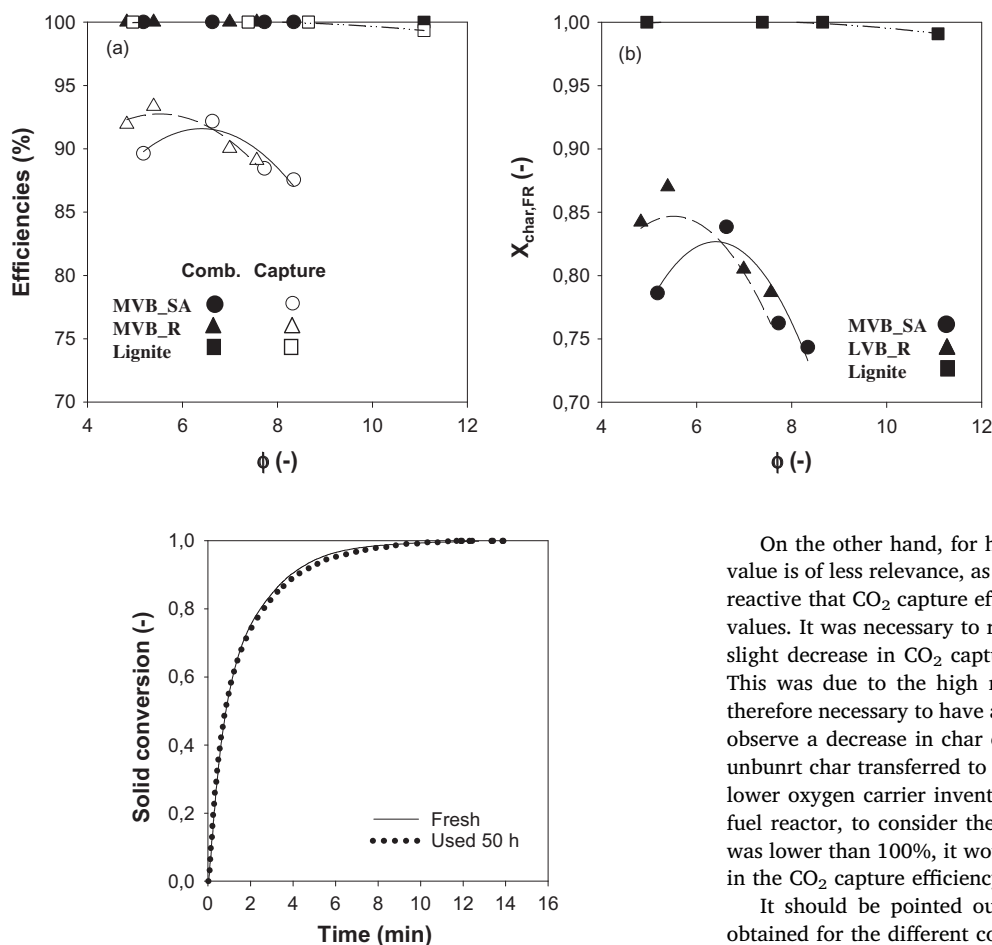

Fig. 4. Conversion vs time curves for oxygen uncoupling reaction for fresh and used particles. Reduction in N_2 and oxidation in air at 950 °C in TGA.

in the oxygen circulation rate had a negative effect on the CO_2 capture effect due to the increase in the unconverted char transferred to the air reactor [10]. However, for both medium volatile coals a maximum was found. At low ϕ values, CO_2 capture efficiency increased, reaching a maximum, with a subsequent decrease in CO_2 capture efficiency with ϕ. Under such conditions, the improvement in the oxygen uncoupling process is highly significant as the oxygen carrier is less reduced [22,23]. Both coals have very similar characteristics and the CO_2 capture efficiency maximum was close for both. Maximum CO_2 capture for the South African coal occurred at values of around $\phi = 6.6$, and of $\phi = 5.4$ for the Russian coal; see Fig. 3(a). When ϕ rose above these values, CO_2 capture efficiency decreased due to the fact that the increase in the solids flow transferred to the air reactor was more important than the increase in the O_2 available in the fuel reactor on the amount of unbunrt char exiting the fuel reactor. A maximum in the CO_2 capture was not observed previously with a Cu-based material [10], suggesting that the determination of the oxygen available for the oxygen uncoupling will be critical to achieve high CO_2 capture values for the Cu-Mn material.

Fig. 3(b) shows the evolution with ϕ of char conversion in fuel reactor for the different coals. With ϕ values lower than the maximum, when ϕ increased, char conversion increased because the oxygen carrier was able to release more gaseous oxygen. However at the same time, the residence time of char particles in fuel reactor decreased when ϕ increased. At values above the maximum, this effect was more important than the increase in the average oxygen carrier reactivity, which caused an increase in the amount of char transferred to the air reactor, and thus CO_2 capture efficiency decreased.

On the other hand, for highly reactive coals, such as lignite, the ϕ value is of less relevance, as can be seen in Fig. 3(a). The lignite was so reactive that CO_2 capture efficiency was 100% for a wide interval of ϕ values. It was necessary to reach ϕ values higher than 10 to observe a slight decrease in CO_2 capture efficiency, which decreased to 99.3%. This was due to the high reactivity of the lignite char [11]. It was therefore necessary to have a big decrease in the char residence time to observe a decrease in char conversion and observe an increase in the unbunrt char transferred to the air reactor; see Fig. 3(b). Perhaps with lower oxygen carrier inventories and residence times for solids in the fuel reactor, to consider the case in which the CO_2 capture efficiency was lower than 100%, it would also be possible to observe a maximum in the CO_2 capture efficiency as a function of ϕ [28].

It should be pointed out that the maximum CO_2 capture values obtained for the different coals were higher than 90%, and 100% was achieved for lignite. To increase the maximum values of CO_2 capture efficiencies to over 95% for both medium volatile bituminous coals, it would be necessary to increase the fuel reactor temperature, or to use a carbon stripper to recover the unbunrt char exiting from the fuel reactor to the air reactor, and return it to the fuel reactor to burn the char completely [28].

4.2. Oxygen carrier attrition resistance

After 50 h of continuous operation burning the different rank coals, the oxygen carrier particles were analysed to evaluate their durability. The combined evaluation of the AJI parameter and crushing strength is a good indicator to verify the resistance of the particles [29]. It is very significant that the crushing strength value of the particles was higher than 1, more specifically 1.2, which is a requirement for the suitable operation of an oxygen carrier in fluidized beds [29,30]. In previous works with a Cu-based oxygen carrier in a CLOU continuous unit, the crushing strength of the particles showed a very significant decrease in this value to below 1 after 40 h of operation time [15].

In light of this good particle crushing strength value, the particles were analysed by means of an ASTM standard D5757 method [24] to verify their attrition resistance. The fresh Cu34Mn66-GR particles presented an AJI value of 3%, which increased to 7.7% after 50 h of operation in the continuous unit; see Table 1. This AJI value of the used particles was slightly higher than the reference value to select a scalable material for the fluid catalytic cracking (FCC) process (AJI $\leq$ 5%) [29].

In a previous work, the same oxygen carrier was used in the continuous CLOU unit under other operation conditions, with different fuel reactor temperature and ϕ values. The AJI test and crushing strength analysis were carried out for this batch of oxygen carrier particles. The AJI value after 30 h of operation burning sub-bituminous Chilean coal with low ϕ values ($\phi < 3$) was 16%, and the crushing strength of the
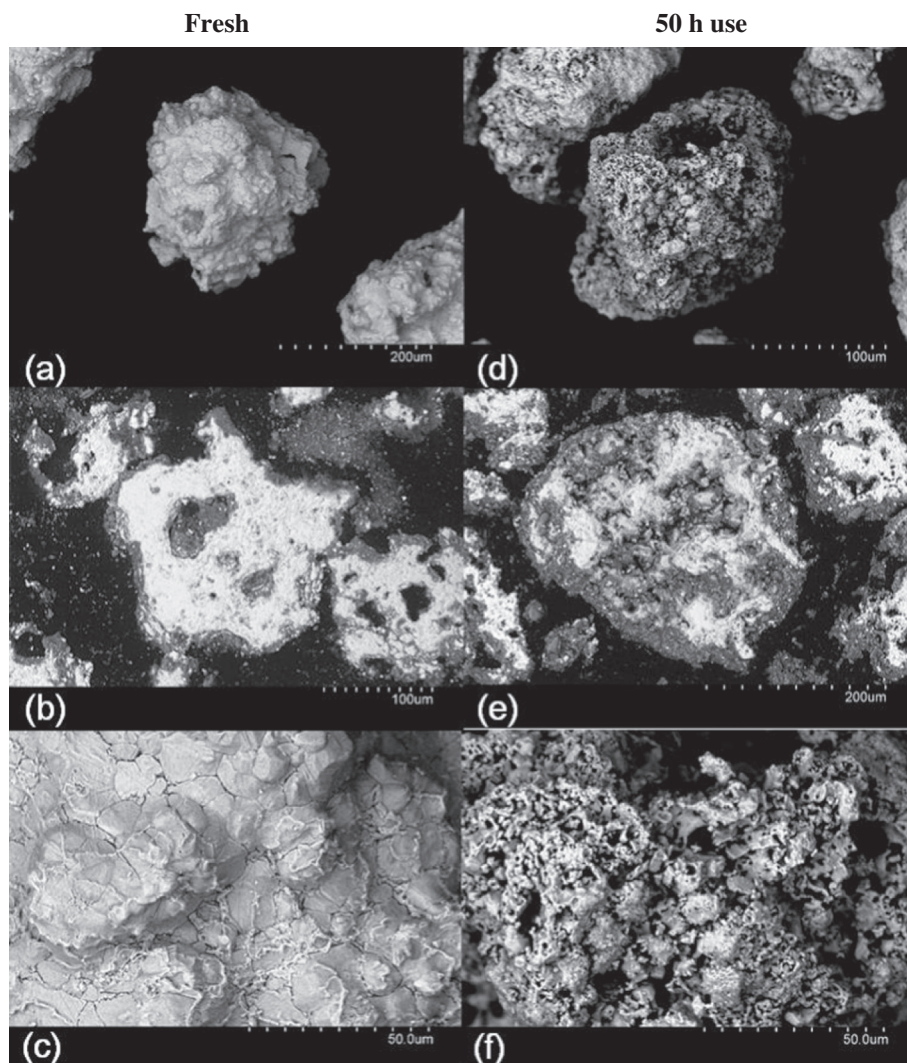
Fresh **50 h use**

Fig. 5. SEM images of fresh (left) and used particles after 50 h in the continuous CLOU unit: (a, d) image of the particles; (b, e) particle cross section; (c, f) surface image of the oxygen carrier particle.

particles was 0.8 N.

This clearly indicates the effect of chemical stress on the attrition rate of oxygen carriers. At low oxygen carrier conversion by the redox process, the attrition rate clearly decreases: AJI = 7.7% when $\phi > 4$, and AJI = 16% when $\phi < 3$. These values correspond to $\Delta X_{oc} < 0.25$ and $\Delta X_{oc} > 0.33$ respectively. Therefore, continuous operation with ϕ values higher than 4 reduces chemical stress and is beneficial for the lifetime of the oxygen carrier particles for the CLOU process.

4.3. Oxygen carrier characterization

Solid samples from the air and fuel reactor were characterized by different techniques after 50 h of continuous operation in the ICB-CSIC-s1 unit. The main properties of the used oxygen carrier particles can be seen in Table 1. It can be seen that the porosity of used particles increased from 12.1 to 18.7% and also appeared to be an increase in the specific surface area, BET. These changes in the particles structure could be associated with the decrease in crushing strength from 1.9 to 1.2.

The XRD analysis of the used particles shows that the main phase was $Cu_{1.5}Mn_{1.5}O_4$, equal to that of the fresh ones. Together with the $Cu_{1.5}Mn_{1.5}O_4$, Mn_3O_4 and a small amount of Mn_2O_3 were detected. Mn_2O_3 was also detected in the experiments in a batch fluidized bed reactor for solid fuels by Adánez-Rubio et al. [22]. Moreover, XRD analysis of the samples showed that the amount of $Cu_{1.5}Mn_{1.5}O_4$ was stable after 50 h of continuous operation.

Reactivity of the oxygen uncoupling step for the fresh and used particles was determined in a TGA at 950 °C, using N_2 during the reduction and air for oxidation. The reactivity data was obtained from the variation in the mass of the sample during the redox cycles as a function of time. The oxygen carrier reduction conversion was calculated as $X_{red} = (m_{ox} - m)/R_{OC} \cdot m_{ox}$, where m is the mass of sample at each time, m_{ox} is the mass of the fully oxidized sample, and R_{OC} is oxygen transport capacity. Fig. 4 shows the oxygen carrier conversion curves for the oxygen release period for fresh and used samples. It can be seen that both reduction reactivity and R_{OC} were maintained by the used oxygen carrier particles, even when a high sulphur content coal (5.2 wt% S in lignite) was evaluated in the CLOU continuous unit.

Fig. 5 shows the SEM images of fresh and used particles after 50 h of continuous operation. In Fig. 5(c and f) it can be seen that after the combustion of coal in the continuous unit, a granular shape was formed on the surface of the particles. This behaviour had previously been observed by Adánez-Rubio et al. [22] using the Cu34Mn66-GR oxygen carrier in batch fluidized bed reactors. They found that this change was enhanced by the increase in the reduction conversion of the particles and could be associated with chemical stress. In Fig. 5(f) it can be seen that this change is more pronounced that in the previous work where the oxygen carrier was only tested in a batch fluidized bed reactor.

5. Conclusions

Complete combustion of different rank coals to CO_2 and H_2O was

achieved in the fuel reactor using a Cu-Mn mixed oxide oxygen carrier (Cu34Mn66-GR) prepared by spray granulation in a spouted bed system. The maximum values of CO_2 capture obtained was 100% for Lignite and 92–93% for both medium volatiles bituminous coals. For both medium volatile coals a maximum CO_2 capture efficiency was reached as a function of the oxygen carrier to fuel ratio, ϕ. The maximum CO_2 capture value for the South African coal was around ϕ = 6.6, and it was ϕ = 5.4 for the Russian coal. For highly reactive coals, such as lignite, ϕ value is of less relevance, and it was necessary to reach ϕ values higher than 10 to observe a slight decrease in CO_2 capture efficiency, which decreased to 99.3%.

After 50 h of continuous operation it was very significant that the value of crushing strength of the particles was higher than 1 N, more specifically 1.2 N. Moreover, the AJI value after 50 h of operation was 7.7%, which is an acceptable value for a scalable CLOU material. Continuous operation with ϕ values higher than 4 is beneficial for the lifetime of the oxygen carrier particles for the CLOU process. This clearly indicates the effect of chemical stress on the attrition rate of oxygen carriers. At low oxygen carrier conversion by the redox process, the attrition rate clearly decreases: AJI = 7.7% at ϕ > 4 and AJI = 16% when ϕ < 3. These values correspond to $\Delta X_{oc} < 0.25$ and $\Delta X_{oc} > 0.33$, respectively.

In summary, the Cu34Mn66-GR oxygen carrier demonstrated very good performance in the combustion of coals of different rank while crushing strength and AJI test values in the used particles were found to be suitable. CO_2 capture efficiencies were higher than 90% at low fuel reactor temperatures (850 °C), and complete combustion of the coals to CO_2 and H_2O was obtained. In order to improve the lifetime of the particles and maximize the CO_2 capture efficiency a value of the oxygen carrier to fuel ratio ϕ = 5–6 is recommended.

Acknowledgements

References

[1] Mattisson T, Lyngfelt A, Leion H. Chemical-looping with oxygen uncoupling for combustion of solid fuels. Int J Greenhouse Gas Control 2009;3:11–9.

[2] Mattisson T. Materials for chemical-looping with oxygen uncoupling. ISRN Chem Eng 2013;2013:19.

[3] Imtiaz Q, Hosseini D, Muller CR. Review of oxygen carriers for chemical looping with oxygen uncoupling (CLOU): thermodynamics, material development, and synthesis. Energy Technol 2013;1:633–47.

[4] Gayán P, Adánez-Rubio I, Abad A, de Diego LF, García-Labiano F, Adánez J. Development of Cu-based oxygen carriers for chemical-looping with oxygen uncoupling (CLOU) process. Fuel 2012;96:226–38.

[5] Adánez-Rubio I, Arjmand M, Leion H, Gayán P, Abad A, Mattisson T, et al. Investigation of combined supports for Cu-based oxygen carriers for chemical-looping with oxygen uncoupling (CLOU). Energy Fuels 2013;27:3918–27.

[6] Pour N, Leion H, Rydén M, Mattisson T. Combined Cu/Mn oxides as an oxygen carrier in chemical looping with oxygen uncoupling [CLOU]. Energy Fuels 2013;27:6031–9.

[7] Hosseini D, Imtiaz Q, Abdala PM, Yoon S, Kierzkowska AM, Weidenkaff A, et al. CuO promoted Mn₂O₃-based materials for solid fuel combustion with inherent CO₂ capture. J Mater Chem A 2015;3:10545–50.

[8] Azimi G, Leion H, Rydén M, Mattisson T, Lyngfelt A. Investigation of different Mn-Fe oxides as oxygen carrier for chemical-looping with oxygen uncoupling [CLOU]. Energy Fuels 2013;27:367–77.

[9] Jing D, Arjmand M, Mattisson T, Rydén M, Snijkers F, Leion H, et al. Examination of oxygen uncoupling behaviour and reactivity towards methane for manganese silicate oxygen carriers in chemical-looping combustion. Int J Greenhouse Gas Control 2014;29:70–81.

[10] Abad A, Adánez-Rubio I, Gayán P, García-Labiano F, de Diego LF, Adánez J. Demonstration of chemical-looping with oxygen uncoupling (CLOU) process in a 1.5 kW_th continuously operating unit using a Cu-based oxygen-carrier. Int J Greenhouse Gas Control 2012;6:189–200.

[11] Adánez-Rubio I, Abad A, Gayán P, de Diego LF, García-Labiano F, Adánez J. Performance of CLOU process in the combustion of different types of coal with CO₂ capture. Int J Greenhouse Gas Control 2013;12:430–40.

[12] Adánez-Rubio I, Abad A, Gayán P, de Diego LF, García-Labiano F, Adánez J. Biomass combustion with CO₂ capture by chemical looping with oxygen uncoupling [CLOU]. Fuel Process Technol 2014;124:104–14.

[13] Adánez-Rubio I, Abad A, Gayán P, García-Labiano F, de Diego LF, Adánez J. The fate of sulphur in the Cu-based chemical looping with oxygen uncoupling (CLOU) process. Appl Energy 2014;113:1855–62.

[14] Pérez-Vega R, Adánez-Rubio I, Gayán P, Izquierdo MT, Abad A, García-Labiano F, et al. Sulphur, nitrogen and mercury emissions from coal combustion with CO₂ capture in chemical looping with oxygen uncoupling [CLOU]. Int J Greenhouse Gas Control 2016;46:28–38.

[15] Adánez-Rubio I, Gayán P, Abad A, de Diego LF, García-Labiano F, Adánez J. Evaluation of a spray-dried CuO/MgAl₂O₄ oxygen carrier for the chemical looping with oxygen uncoupling process. Energy Fuels 2012;26:3069–81.

[16] Shulman A, Cleverstam E, Mattisson T, Lyngfelt A. Manganese/iron, manganese/nickel, and manganese/silicon oxides used in chemical-looping with oxygen uncoupling (CLOU) for combustion of methane. Energy Fuels 2009;23:5269–75.

[17] Mei D, Mendiara T, Abad A, De Diego LF, García-Labiano F, Gayán P, et al. Evaluation of manganese minerals for chemical looping combustion. Energy Fuels 2015;29:6605–15.

[18] Sundqvist S, Arjmand M, Mattisson T, Rydén M, Lyngfelt A. Screening of different manganese ores for chemical-looping combustion [CLC] and chemical-looping with oxygen uncoupling (CLOU). Int J Greenhouse Gas Control 2015;43:179–88.

[19] Azad AM, Hedayati A, Rydén M, Leion H, Mattisson T. Examining the Cu–Mn–O spinel system as an oxygen carrier in chemical looping combustion. Energy Technol 2013;1:59–69.

[20] Xu L, Edland R, Li Z, Leion H, Zhao D, Cai N. Cu-modified manganese ore as an oxygen carrier for chemical looping combustion. Energy Fuels 2014;28:7085–92.

[21] Adánez-Rubio I, Abad A, Gayán P, Adánez I, de Diego LF, García-Labiano F, et al. Use of hopcalite-derived Cu-Mn mixed oxide as oxygen carrier for chemical looping with oxygen uncoupling process. Energy Fuels 2016;30:5953–63.

[22] Adánez-Rubio I, Izquierdo MT, Abad A, Gayan P, de Diego LF, Adánez J. Spray granulated Cu-Mn oxygen carrier for chemical looping with oxygen uncoupling (CLOU) process. Int J Greenhouse Gas Control 2017;65:76–85.

[23] Adánez-Rubio I, Gayan P, Abad A, de Diego LF, García-Labiano F, Adánez J. Coal combustion with a spray granulated Cu-Mn mixed oxide for the Chemical Looping with Oxygen Uncoupling (CLOU) process. Appl Energy 2017. http://dx.doi.org/10.1016/j.apenergy.2017.09.098.

[24] ASTM. Standard test method for determination of attrition and abrasion of powdered catalyst by air jets, Standard Test Method for Determination of Attrition and Abrasion of Powdered Catalysts by Air Jets; 2011.

[25] Zafar Q, Abad A, Mattisson T, Gevert B, Strand M. Reduction and oxidation kinetics of Mn₃O₄/Mg-ZrO₂ oxygen carrier particles for chemical-looping combustion. Chem Eng Sci 2007;62:6556–67.

[26] Driessens FCM, Rieck GD. Phase equilibria in the system Cu-Mn-O. Z Anorgan Allgemeine Chem 1967;351.

[27] Abad A, Adánez J, García-Labiano F, de Diego LF, Gayán P, Celaya J. Mapping of the range of operational conditions for Cu-, Fe-, and Ni-based oxygen carriers in chemical-looping combustion. Chem Eng Sci 2007;62:533–49.

[28] Adánez-Rubio I, Gayán P, Abad A, García-Labiano F, de Diego LF, Adánez J. Kinetic analysis of a Cu-based oxygen carrier: relevance of temperature and oxygen partial pressure on reduction and oxidation reactions rates in chemical looping with oxygen uncoupling (CLOU). Chem Eng J 2014;256:69–84.

[29] Cabello A, Gayán P, García-Labiano F, de Diego LF, Abad A, Adánez J. On the attrition evaluation of oxygen carriers in chemical looping combustion. Fuel Process Technol 2016;148:188–97.

[30] Rydén M, Moldenhauer P, Lindqvist S, Mattisson T, Lyngfelt A. Measuring attrition resistance of oxygen carrier particles for chemical looping combustion with a customized jet cup. Powder Technol 2014;256:75–86.